1986

Determination of far-field stress from localized stress concentrations

John Robert Rohde
Iowa State University

Rohde, John Robert

DETERMINATION OF FAR-FIELD STRESS FROM LOCALIZED STRESS CONCENTRATIONS

Iowa State University PH.D. 1986

PLEASE NOTE:

In all cases this material has been filmed in the best possible way from the available copy. Problems encountered with this document have been identified here with a check mark __✓__.

1. Glossy photographs or pages _____
2. Colored illustrations, paper or print _____
3. Photographs with dark background _____
4. Illustrations are poor copy _____
5. Pages with black marks, not original copy _____
6. Print shows through as there is text on both sides of page _____
7. Indistinct, broken or small print on several pages ✓
8. Print exceeds margin requirements _____
9. Tightly bound copy with print lost in spine _____
10. Computer printout pages with indistinct print _____
11. Page(s) _____ lacking when material received, and not available from school or author.
12. Page(s) _____ seem to be missing in numbering only as text follows.
13. Two pages numbered _____. Text follows.
14. Curling and wrinkled pages _____
15. Dissertation contains pages with print at a slant, filmed as received _____
16. Other _____

_____

_____

University
Microfilms
International

Determination of far-field stress from localized stress concentrations

by

John Robert Rohde

A Dissertation Submitted to the
Graduate Faculty in Partial Fulfillment of the
Requirements for the Degree of
DOCTOR OF PHILOSOPHY

Department: Civil Engineering
Major: Geotechnical Engineering

Approved:

Signature was redacted for privacy.

In Charge of Major Work

Signature was redacted for privacy.

For the Major Department

Signature was redacted for privacy.

For the Graduate College

Iowa State University
Ames, Iowa

1986

TABLE OF CONTENTS

LIST OF FIGURES

LIST OF TABLES

ABSTRACT

The purpose of this work was to develop a method of determining far-field principal stress magnitude and orientation using biaxial stress measurements made in a series of bore holes. Two novel developments were employed: one was a method for relating biaxial measurements from three bore holes to the triaxial principal stress field; the other was a measurement technique that fully defines the biaxial stress field around a bore hole, independent of rock properties. To determine the triaxial principal stress field, a series of simultaneous equations describing biaxial measurements in terms of a random baseline coordinate system was developed. A least squares regression was then utilized to determine the coordinate system's stress field. A Newton-Raphson reduction was subsequently performed to define the orientation and magnitude of the principal stress field. The biaxial stress measurement technique employs two loading mechanisms and ultrasonic crack detection. The biaxial stress field in bore holes with nonhomogeneous and anisotropic rock conditions can be defined. Finally, recommendations are given for the development of a testing apparatus utilizing thin-film piezoelectric substrates to detect ultrasonic shear waves capable of underground biaxial measurements.

INTRODUCTION

By determining the true undisturbed principal stress field in a rock mass, theories of elasticity and plasticity can be applied to determine the actual stresses exerted on an underground opening. Unfortunately, the act of measuring in situ stress reorients the natural stress field, limiting in situ stress determination techniques to measurements in a disturbed field. The stress measurement theory here developed provides a method by which existing or far-field stress conditions can be determined from reoriented biaxial stress data measured in three bore holes. Stress transformation techniques based on the geometries and the biaxial fields of the bore holes are utilized to determine the natural stress field prior to the introduction of the bore holes.

A new technique for biaxial stress measurement was developed, induced fracture; this technique is unique in its ability to determine biaxial stresses in bore holes containing preexisting fractures and under anisotropic rock conditions. Induced fracture employs active fracturing using two loading devices. Fractures are identified ultrasonic crack detection. The first load device is a radial stress device which, when pressurized, causes a crack oriented parallel to the biaxial major principal stress under isotropic and homogeneous conditions. The second device is a line load device applied in the direction of the initial fracture providing information needed to calculate the magnitude of the biaxial principal stress field acting on the bore hole.

The combination of the new stress measurement theory developed in this study with the induced fracture technique provides a method by which the true principal stress field may be determined independent of material properties. Induced fracture, combined with various loading schemes, also provides for biaxial stress determination in a single bore hole under anisotropic and nonhomogeneous conditions. This is not possible with existing bore hole stress determination techniques.

BACKGROUND

In Situ Stress

Traditional theories derive vertical stress from the weight of the overburden. The resultant horizontal stress is the stress required to resist horizontal deformation and is calculated from Poisson's ratio and the assumption of elasticity. Two major problems arise from the traditional approach: it is difficult to accurately determine Poisson's ratio; also, the predicted relationship between horizontal and vertical stress has been shown to be incorrect. Recent measurements at depths of less than seven thousand feet have shown, contrary to classical prediction, that horizontal stress is greater than vertical stress. Friedman (1972) attributes this high level of horizontal stress to residual elastic strains reflecting past geologic loading. Other possible factors include tectonic, hydrodynamic, and thermal activities which may contribute to both vertical and horizontal stresses.

In Situ Stress Measurement

Numerous experimental techniques have been developed to measure in situ stress: some measure stress change, others determine absolute stresses. These various techniques fall into two general categories, active and passive. Active test instruments employ some loading technique to determine in situ stress. Passive techniques generally measure

strain upon stress relief and use elastic properties of the rock to calculate in situ stress; these elastic properties are determined independently of the test.

Active techniques

Two active test instruments commonly used to determine in situ stresses are hydraulic fracture and flat-jack devices. In addition, a new technique, active fracturing, has recently been developed at Iowa State University (Pitt and Klostermann, 1984). Hydraulic fracturing is a bore hole technique in which two packers are placed in a bore hole; pressure is then increased between the packers until a drop in pressure under constant flow is noted, indicating the formation of a crack. The maximum pressure under constant flow is defined as the sum of the tensile strength of the rock plus the minimum stress concentration of the biaxial stress field caused by the bore hole. To determine the minimum stress concentration, the pressure between the packers is increased a second time. The peak pressure achieved is defined as the minimum stress concentration without the tensile strength component, because the rock had been previously fractured. The constant pressure maintained after initial peak load for both pressurizations is defined as the biaxial minor principal stress. The two values (minimum stress concentration and minor principle stress) derived from the test sequence allow calculation of the biaxial principal stress field surrounding the bore hole, as well as the tensile strength of the rock. An oriented impression packer is required

to determine the direction of the crack, which coincides with the major principal stress (Hubbert and Willis, 1957).

Flat-jack techniques are based on the principle of replacing the in situ stress with hydraulic pressure. The test is accomplished either by placing deformation measuring instruments on the desired surfaces to establish a pre-installation position, or by using bore hole inclusion stress meters to establish a preinstallation state of stress. A notch is then cut and a flat-jack is grouted into place. The in situ stress prior to flat-jack insertion is defined as the pressure required within the flat-jack to either return the deformation to zero, or to reestablish the initial pressure reading on the bore hole inclusion stress meter.

A recently-developed technique (Klostermann, 1984) rapidly evaluates the biaxial stress field acting on a bore hole. The technique employs a loading mechanism and a system for crack detection. The loading device is a hollow rubber cylinder with a rod running through the center; a hollow hydraulic cylinder is then used to squeeze the rubber between two end caps, applying radial stress to the bore hole wall. To detect the resulting failure, ultrasonic compression wave travel time is measured around the free surface of the biaxially loaded bore hole.

The test sequence is divided into two discrete phases. In the first phase, a bore hole is drilled; the rubber cylinder then is placed in the hole, and the ultrasonic probes then are placed on either side. Pressure is applied to the hollow-core cylinder until a change in ultrasonic travel time is detected. This pressure level is defined as the radial stress required to overcome the tensile strength of the material and the

minimum stress concentration on the bore hole wall. Pressure is released and then reapplied, again using the ultrasonic travel time measurements, to determine the minimum stress concentration by reopening the existing crack without the influence of tensile strength. After determining the orientation of the initial crack (in theory parallel to the major principal biaxial compressive stress) the second phase of the test is initiated by boring a second bore hole adjacent to the first and tangential to the initially formed crack. A second radial stress device is then inserted in the new bore hole and the ultrasonic travel time measurements are performed across the gap between the holes. The two radial stress devices are simultaneously pressurized, causing a stress concentration between the holes, until a change in the ultrasonic travel time is noted. The radial pressure measured at this point is defined as the tensile strength of the material plus the stress concentration resulting from the two-hole configuration. The pressure is released and then reapplied to determine the stress concentration independent of the tensile strength.

Combining the results from the one- and two-hole tests allows calculation of the biaxial principal stress field surrounding the bore hole.

Testing of this measurement scheme was performed in cement mortar blocks under known biaxial loads. Results from testing were encouraging, predicting the applied stress to within 20 percent, a level equal to or better than existing methods.

The method is promising, but the two-hole aproach limits it to near-surface applications. Precise hole spacing is required to determine stress concentration in the two-hole test.

Passive techniques

The major tests for passive measurement of in situ stress in a bore hole can be classified into three categories (Leeman, 1964): deformation strain cells, inclusion stress meters, and strain gage devices. After one of these devices is placed within a bore hole, the regional stresses are removed by overcoring. The initial stress level around the bore hole then can be determined through displacements measured with deformation gages, or by stress changes monitored with inclusion stress meters. Independently determined elastic rock properties are used with either technique.

Summation

In general, all techniques except hydraulic fracturing are limited to near-surface measurements by the complexity of the drilling procedures required (Leeman, 1964). Flat-jack techniques using deformation are restricted to on-wall testing. Bore hole inclusion stress meter tests have been performed at 20-foot depths (Leeman, 1964); to achieve these depths, extensive drilling and difficult grouting is required. Flat-jack tests require several weeks for the grout to set and the deformation to stabilize before the test is complete. Bore hole deformation techniques are generally limited to depths of 30 to 50 feet, and again, are time-consuming because of the drilling required. Also, the drilling requirements for active fracturing limit its use to near-surface applications.

Hydraulic fracturing is not restricted to shallow depths, but its uses are limited to nonporous, unbroken and isotropic rock. The fracture orientation of the hydraulically induced fracture is often hard to determine using impression packers (Bredehoeft et al., 1976; Haimson, 1975), and the variability encountered in testing makes the tests difficult to reproduce and interpret (Panek, 1984).

Therefore, one may observe, as a general conclusion, that existing methods for measurement of in situ stress either are limited in application or are prohibitively expensive for regular use. All test methods except some of the complex stress relief techniques were developed to measure the biaxial stress field around a bore hole, making the global assumption that one principal stress direction is parallel to the bore hole. Working near a free surface assures the validity of this assumption; at greater depths, however, the assumption becomes questionable because the orientation of the principal stress field is unknown. Therefore, a method which predicts the true principal stress field would be valuable to assess the actual in situ stress orientation and magnitude.

DEVELOPMENT OF FAR-FIELD STRESS RELATIONSHIPS

Two different formats will be developed to determine the far-field principal stresses. The first is a simple theory, primarily for explanation; the second is more general. The first theory involves direct measurement of biaxial stresses upon three mutually perpendicular axes and the transformation of these axes to determine the principal stress field. The second theory utilizes triaxial stress transformation to determine the principal stress field from biaxial stress measurements made in randomly oriented bore holes.

Fixed Bore Hole Orientation

For this determination, bore holes are drilled from an underground opening along three mutually perpendicular axes, as shown in Figure 1. The bore holes are assumed to be of sufficient depth to escape the effects of the opening, and the stress field is relatively constant. This construction implies that one principal stress direction is vertical. Localized biaxial principal stresses can then be determined, as shown in Figure 1, for the y-axis. The localized principal stress field, σ_{1y} and σ_{2y}, and the angle from the z axis to σ_{1y}, can be transformed using

$$\sigma_z = \frac{\sigma_{1y} + \sigma_{2y}}{2} + \frac{\sigma_{1y} - \sigma_{2y}}{2}\cos 2\theta \qquad (1)$$

$$\sigma_x = \frac{\sigma_{1y} + \sigma_{2y}}{2} + \frac{\sigma_{1y} - \sigma_{2y}}{2}\cos 2(\theta + \pi/2) \qquad (2)$$

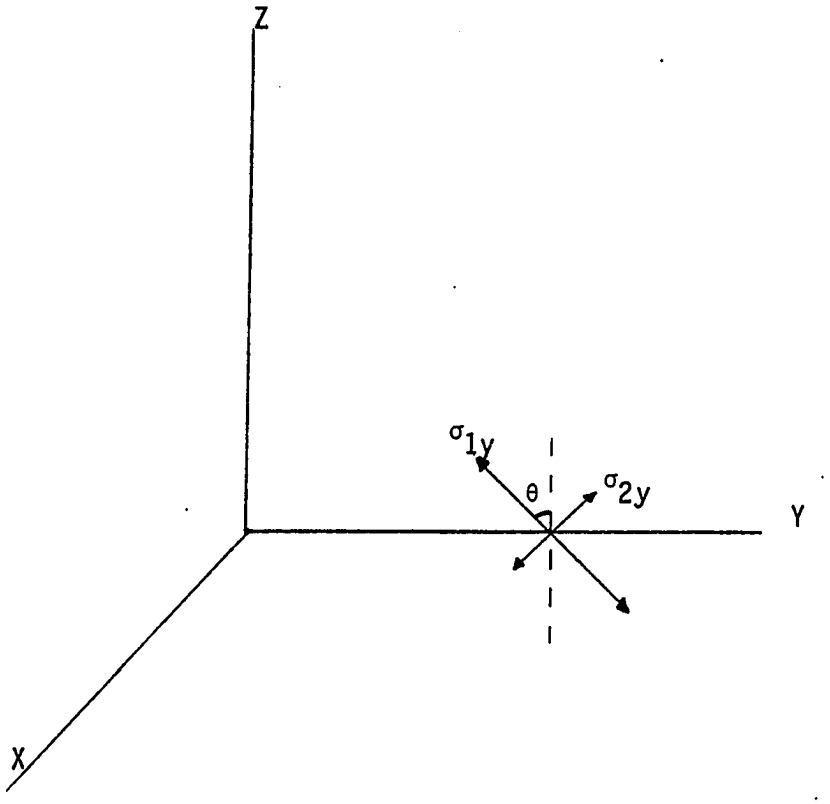

Figure 1: Stress determination in a fixed hole orientation

$$\tau_{zx} = -\frac{\sigma_{1y} - \sigma_{2y}}{2}\sin 2\theta \qquad (3)$$

to reflect the stresses on the xyz axis. Tests performed along the x and z axes, where β is the angle from the x axis to σ_{1z} and α is the angle from the y axis to σ_{1x}, can be transformed using:

$$\sigma_x = \frac{\sigma_{1z} + \sigma_{2z}}{2} + \frac{\sigma_{1z} - \sigma_{2z}}{2}\cos 2\beta \qquad (4)$$

$$\sigma_y = \frac{\sigma_{1z} + \sigma_{2z}}{2} + \frac{\sigma_{1z} - \sigma_{2z}}{2}\cos 2(\beta + \pi/2) \qquad (5)$$

$$\tau_{xy} = -\frac{\sigma_{1z} - \sigma_{2z}}{2}\sin 2\beta \qquad (6)$$

$$\sigma_y = \frac{\sigma_{1x} + \sigma_{2x}}{2} + \frac{\sigma_{1x} - \sigma_{2x}}{2}\cos 2\alpha \qquad (7)$$

$$\sigma_z = \frac{\sigma_{1x} + \sigma_{2x}}{2} + \frac{\sigma_{1x} - \sigma_{2x}}{2}\cos 2(\alpha + \pi/2) \qquad (8)$$

$$\sigma_{yz} = -\frac{\sigma_{1x} - \sigma_{2x}}{2}\sin 2\alpha. \qquad (9)$$

The determination of the magnitude and orientation of the principal stress field is then accomplished by solving:

$$i^3 - I_1 i^2 + I_2 i - I_3 = 0 \quad (i=1,2,3) \qquad (10)$$

where the three roots are real and

$$I_1 = \sigma_x + \sigma_y + \sigma_z \qquad (11)$$

$$I_2 = -(\sigma_x\sigma_y + \sigma_y\sigma_z + \sigma_z\sigma_x) + \tau_{xy}^2 - \tau_{yz}^2 - \tau_{zx}^2 \qquad (12)$$

$$I_3 = \sigma_x\sigma_y\sigma_z - \sigma_x\tau_{yz}^2 - \sigma_y\tau_{zx}^2 - \sigma_z\tau_{xy}^2 + 2\tau_{xy}\tau_{yz}\tau_{zx}. \qquad (13)$$

The orientation of the principal planes (σ_1, σ_2 and σ_3) subsequently can be determined by:

$$\cos(\sigma_i,x) = A_i/K_i \tag{14}$$

$$\cos(\sigma_i,y) = B_i/K_i \tag{15}$$

$$\cos(\sigma_i,z) = C_i/K_i \tag{16}$$

where $$K_i = (A_i^2 + B_i^2 + C_i^2)^{1/2} \tag{17}$$

$$A_i = (\sigma_y - \sigma_i)(\sigma_z - \sigma_i) - \tau_{xy}^2 \tag{18}$$

$$B_i = \tau_{zy}\tau_{xy} - \tau_{xy}(\sigma_z - \sigma_i) \tag{19}$$

$$C_i = \tau_{xy}\tau_{yz} - \tau_{xz}(\sigma_y - \sigma_i) \tag{20}$$

and $\cos(\sigma_i,x)$, $\cos(\sigma_i,y)$, and $\cos(\sigma_i,z)$ are the cosines of the angles formed between the determined principal stress axis and the corresponding original axis.

This reduction provides an additional value for σ_x, σ_y and σ_z that reflects the accuracy of the test procedures. These additional values could be used to provide inputs for a least squares reduction in order to improve the quality of the results. Since it is impractical to drill along three mutually perpendicular axes, a more general reduction technique with greater applicability would be of more value.

Random Bore Hole Orientation

Stress around a bore hole

To determine the localized stress field around a bore hole, it is necessary to consider the stress field prior to drilling. This requires

an understanding of three-dimensional transformations of a randomly oriented stress field. The stress on an element is defined by:

$$\sigma_{x'} = \sigma_x\cos^2(x',x) + \sigma_y\cos^2(x',y) + \sigma_z\cos^2 x',z) \tag{21}$$
$$+ 2\tau_{xy}\cos(x',y)\cos(x',x) + 2\tau_{yz}\cos(x',z)\cos(x',y)$$
$$+ 2\tau_{zx}\cos(x',x)\cos(x',z)$$

$$\tau_{x'y'} = \sigma_x\cos(x',x)\cos(y',x) + \sigma_y\cos(x',y)\cos(y',y) \tag{22}$$
$$+ \sigma_z\cos(x',z)\cos(y',z)$$
$$+ \tau_{xy}(\cos(x',y)\cos(y',x) + \cos(x',x)\cos(y',y))$$
$$+ \tau_{yz}(\cos(x',z)\cos(y',y) + \cos(x',y)\cos(y',z))$$
$$+ \tau_{zx}(\cos(x',x)\cos(y',z) + \cos(x',z)\cos(y',x))$$

$$\sigma_{y'} = \sigma_x\cos^2(y',x) + \sigma_y\cos^2(y',y) + \sigma_z\cos^2(y',z) \tag{23}$$
$$+ 2\tau_{xy}\cos(y',x)\cos(y',y) + 2\tau_{yz}\cos(y',y)\cos(y'z)$$
$$+ 2\tau_{zx}\cos(y',z)\cos(y',x)$$

$$\tau_{y'z'} = \sigma_x\cos(y',x)\cos(z',x) + \sigma_y\cos(y',y)\cos(z',y) \tag{24}$$
$$+ \sigma_z\cos(y',z)\cos(z',z)$$
$$+ \tau_{xy}(\cos(y',y)\cos(z',x) + \cos(y',x)\cos(z',y))$$
$$+ \tau_{yz}(\cos(y',z)\cos(z',y) + \cos(y',y)\cos(z',z))$$
$$+ \tau_{zx}(\cos(y',x)\cos(z',z) + \cos(y',z)\cos(z',x))$$

$$\sigma_{z'} = \sigma_x\cos^2(z',x) + \sigma_y\cos^2(z',y) + \sigma_z\cos^2(z',z) \tag{25}$$
$$+ 2\tau_{xy}\cos(z',y)\cos(z',x) + 2\tau_{yz}(\cos(z',z)\cos(z',y)$$
$$+ 2\tau_{zx}\cos(z',x)\cos(z',z)$$

$$\tau_{z'x'} = \sigma_x\cos(z',x)\cos(x',x) + \sigma_y\cos(z',y)\cos(x',y) \quad (26)$$
$$+ \sigma_z\cos(z',z)\cos(x',z)$$
$$+ \tau_{xy}(\cos(z',y)\cos(x',x) + \cos(z',x)\cos(x',y))$$
$$+ \tau_{yz}(\cos(z',z)\cos(x',y) + \cos(z',y)\cos(x',z))$$
$$+ \tau_{zx}(\cos(z',x)\cos(x',z) + \cos(z',z)\cos(x',x))$$

where the cosine terms represent the angles between the referenced axes (Ford and Alexander, 1977).

After defining the localized stress field, it is necessary to determine its influence on the stress concentrations surrounding the bore hole. A complete definition is available from Fairhurst (1965); for the present purposes, only the localized stress influencing the tangential stress will be considered. From Figure 2, the influences on tangential stress are:

$$\sigma_\theta = \sigma_x + \sigma_y - 2(\sigma_x-\sigma_y)\cos2\theta - 4\tau_{xy}\sin2\theta \quad (27)$$

where all other effects are zero. Obviously, the localized stress field surrounding the bore hole acts as a biaxial field; however, it is important to remember that this biaxial field is a distinct transformation of far-field stress.

The two-dimensional transformation of the measured localized biaxial principal stress field surrounding the bore hole to the desired geometry also is important. From a given set of biaxial principal stresses, σ_1 and σ_2, and an angle β, the biaxial stress field can be defined as:

$$\sigma_{1,2} = \sigma_{x2}\cos^2\beta + \sigma_y\sin^2\beta \quad (28)$$

$$\tau_{xy} = \tfrac{1}{2}(\sigma_2 - \sigma_1)\sin2\beta. \quad (29)$$

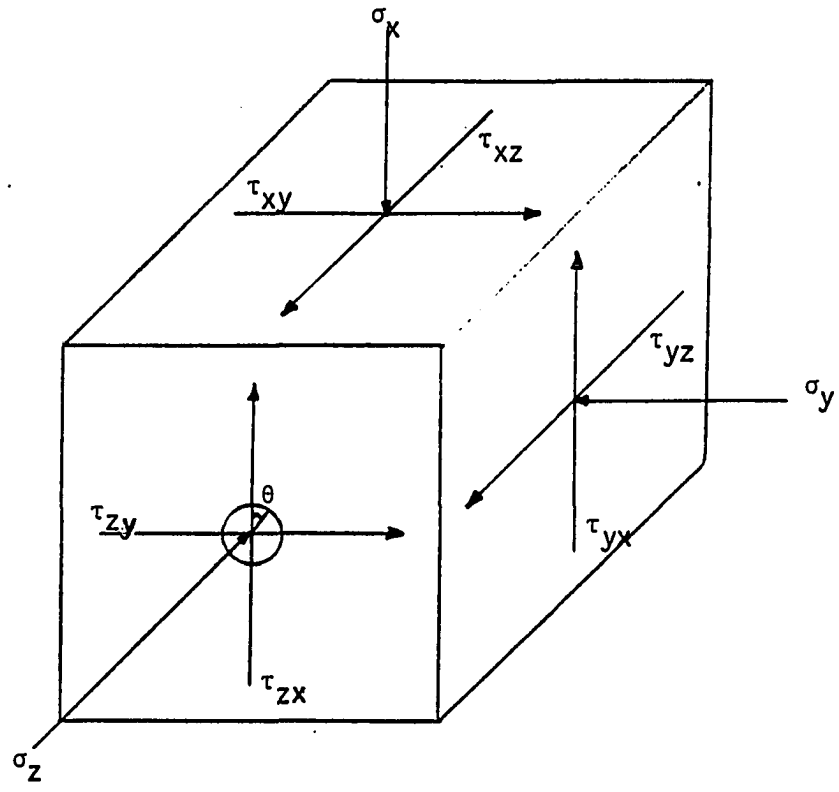

Figure 2: Stress concentations due to a triaxial stress field

Examination of the relationships set forth in Equations 21-29 shows that a bore hole and the subsequently determined biaxial stress field can be related by direction cosines to a base coordinate system. The magnitude of the biaxial principal stress field can be used to develop three equations, incorporating six unknowns, these being the stress field acting on the randomly chosen base coordinate system.

To implement the transformation in an underground environment, it is important to establish a workable geometry. While direction cosines are adequate for theoretical development, they are too complex to determine in the field. If a baseline coordinate system were established using the directions east, north and "up" for σ_x, σ_y and σ_z, respectively, a spherical coordinate system would provide a suitable geometry. Using spherical coordinates (Figure 3), the axis of the bore hole, z', is defined by the angles λ and θ. If the orientation of the x' reflection on the xy plane is constrained to the direction defined by λ, a full set of direction cosines is defined by:

$$\cos(x',x) = \cos\theta\cos\lambda \tag{30}$$

$$\cos(x',y) = \cos\theta\sin\lambda \tag{31}$$

$$\cos(x',z) = -\sin\theta \tag{32}$$

$$\cos(y',x) = -\sin\lambda \tag{33}$$

$$\cos(y',y) = \cos\lambda \tag{34}$$

$$\cos(y',z) = 0 \tag{35}$$

$$\cos(z',x) = \sin\theta\cos\lambda \tag{36}$$

$$\cos(z',y) = \sin\theta\sin\lambda \tag{37}$$

$$\cos(z',z) = \cos\theta. \tag{38}$$

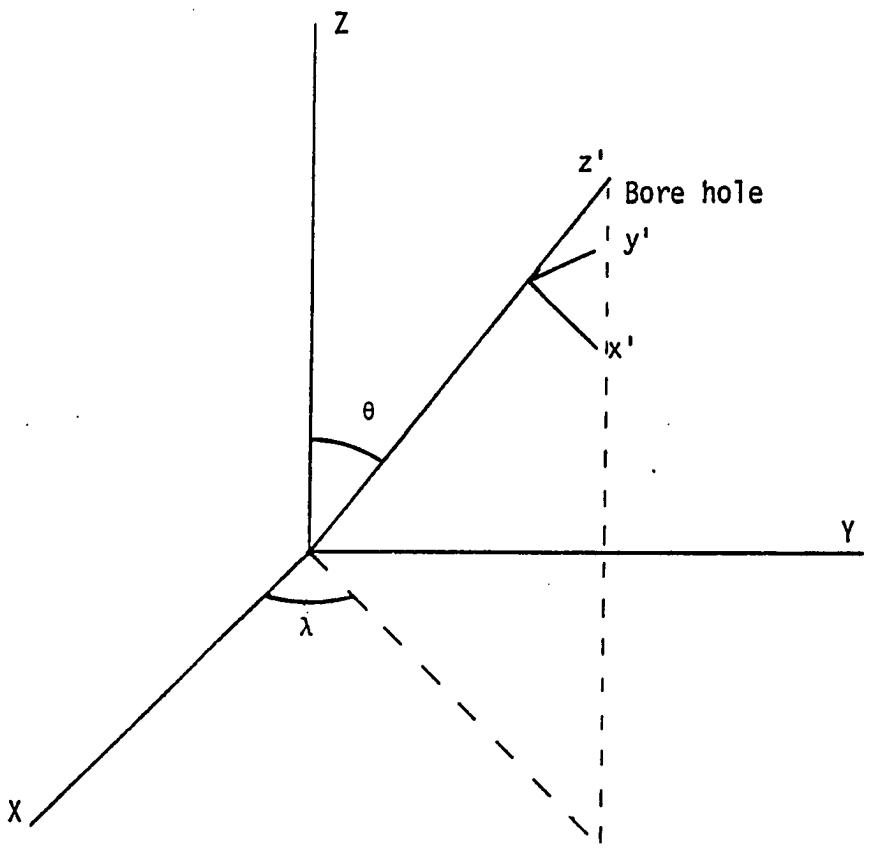

Figure 3: Spherical coordinate system

To utilize these direction cosines, the measured biaxial principal stresses in the bore hole are transformed about the z' axis, using Equations 28 and 29, to determine σ_x', σ_y' and σ_{xy}'.

Bore hole transformation

If a hypothetical test sequence were performed from an underground or a surface location, an appropriate baseline coordinate system would be east, north, and "up" for x, y, and z, respectively. The first bore hole could then be drilled as shown in Figure 4. The angles from the bore hole to the three baseline axes (θ,λ) define the direction cosines $\cos(z',x)_1$, $\cos(z',y)_1$, and $\cos(z',z)_1$. A test is then performed to determine the localized biaxial principal stresses and their directions. The principal stresses shown in Figure 4 then can be transformed to the directions defined by the direction cosines $(\cos(x',x)_1$, $\cos(x',y)_1$, $\cos(x',z)_1$ for $\sigma x'_1$ and $\cos(y'x)_1$, $\cos(y'y)_1$, and $\cos(y'z)_1$ for $\sigma_y'1$. Using the magnitudes of the biaxial principal stresses ($\sigma x'1$ $\sigma y'1$ and $\sigma xy'1$), the following relationships define the transformed biaxial stresses in terms of the baseline coordinate system,

$$\sigma_{x'1} = \sigma_x\cos^2(x',x)_1 + \sigma_y\cos^2(x',y)_1 + \sigma_z\cos^2(x',z)_1 + 2\tau_{xy}\cos(x',y)_1\cos(x',x)_1 + 2\tau_{yz}\cos(x',z)_1\cos(x',y)_1 + 2\tau_{zx}\cos(x',x)_1\cos(x',z)_1 \quad (39)$$

$$\sigma_{y'1} = \sigma_x\cos^2(y',x)_1 + \sigma_y\cos^2(y',y)_1 + \sigma_z\cos^2(y',z)_1 + 2\tau_{xy}\cos(y',x)_1\cos(y',y)_1 + 2\tau_{yz}\cos(y',y)_1\cos(y',z)_1 + 2\tau_{zx}\cos(y',z)_1\cos(y',x)_1 \quad (40)$$

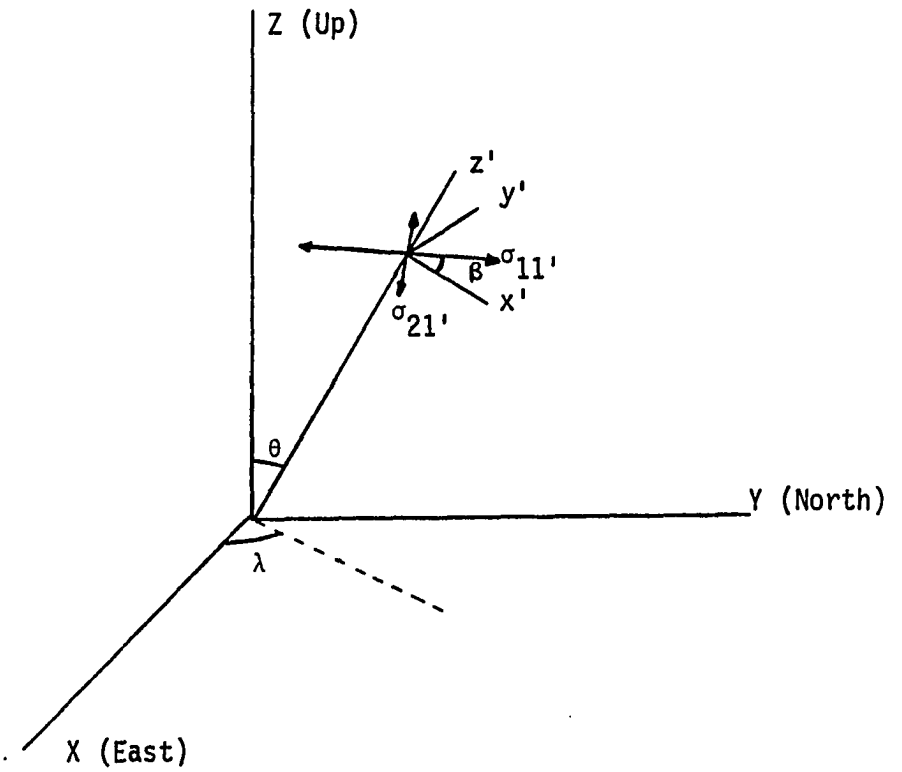

Figure 4: Relation of bore hole to baseline coordinate system

$$\tau_{xy'1} = \sigma_x\cos(x',x)_1\cos(y',x)_1 + \sigma_y\cos(x',y)_1\cos(y',y)_1 \quad (41)$$
$$+ \sigma_z\cos(x',z)_1\cos(y',z)_1$$
$$+ \tau_{xy}(\cos(x',y)_1\cos(y',x)_1 + \cos(x',x)_1\cos(y',y)_1)$$
$$+ \tau_{yz}(\cos(x',z)_1\cos(y',y)_1 + \cos(x',y)_1\cos(y',z)_1)$$
$$+ \tau_{zx}(\cos(x',x)_1\cos(y',z)_1 + \cos(x',z)_1\cos(y',x)_1)$$

where σ_x, σ_y, σ_z, τ_{xy}, τ_{yz} and τ_{zx} are the unknown magnitudes of the baseline stress field.

A second bore hole drilled in a different orientation can be treated identically to develop,

$$\sigma_{x'2} = \sigma_x\cos^2(x',x)_2 + \sigma_y\cos^2(x',y)_2 + \sigma_z\cos^2(x',z)_2 \quad (42)$$
$$+ 2\tau_{xy}\cos(x',y)_2\cos(x',x)_2 + 2\tau_{yz}\cos(x',z)_2\cos(x',y)_2$$
$$+ 2\tau_{zx}\cos(x',x)_2\cos(x',z)_2$$

$$\sigma_{y'2} = \sigma_x\cos^2(y',x)_2 + \sigma_y\cos^2(y',y)_2 + \sigma_z\cos^2(y',z)_2 \quad (43)$$
$$+ 2\tau_{xy}\cos(y',x)_2\cos(y',y)_2 + 2\tau_{yz}\cos(y',y)_2\cos(y',z)_2$$
$$+ 2\tau_{zx}\cos(y',z)_2\cos(y',x)_2$$

$$\tau_{xy'2} = \sigma_x\cos(x',x)_2\cos(y',x)_2 + \sigma_y\cos(x',y)_2\cos(y',y)_2 \quad (44)$$
$$+ \sigma_z\cos(x',z)_2\cos(y',z)_2$$
$$+ \tau_{xy}(\cos(x',y)_2\cos(y',x)_2 + \cos(x',x)_2\cos(y',y)_2)$$
$$+ \tau_{yz}(\cos(x',z)_2\cos(y',y)_2 + \cos(x',y)_2\cos(y',z)_2)$$
$$+ \tau_{zx}(\cos(x',x)_2\cos(y',z)_2 + \cos(x',z)_2\cos(y',x)_2)$$

for a total of six equations and six unknowns.

The solution matrix of the six simultaneous equations is singular showing that the equations are not completely independent. Therefore, a third test is required to completely determine the stress field on the baseline coordinate system.

A biaxial test in a third bore hole provides three additional relationships,

$$\sigma_{x'3} = \sigma_x \cos^2(x',x)_3 + \sigma_y \cos^2(x',y)_3 + \sigma_z \cos^2(x',x)_3 \quad (45)$$
$$+ 2\tau_{xy}\cos(x',y)_3\cos(x',x)_3 + 2\tau_{yz}\cos(x',z)_3\cos(x',y)_3$$
$$+ 2\tau_{zx}\cos(x',x)_3\cos(x',z)_3$$

$$\sigma_{y'3} = \sigma_x \cos^2(y',x)_3 + \sigma_y \cos^2(y',y)_3 + \sigma_z \cos^2(y',z)_3 \quad (46)$$
$$+ 2\tau_{xy}\cos(y',x)_3\cos(y',y)_3 + 2\tau_{yz}\cos(y',y)_3\cos(y',z)_3$$
$$+ 2\tau_{zx}\cos(y',z)_3\cos(y',x)_3$$

$$\tau_{xy'3} = \sigma_x \cos(x',x)_3\cos(y',x)_3 + \sigma_y \cos(x',y)_3\cos(y',y)_3 \quad (47)$$
$$+ \sigma_z \cos(x',z)_3\cos(y',z)_3$$
$$+ \tau_{xy}(\cos(x',y)_3\cos(y',x)_3 + \cos(x',x)_3\cos(y',y)_3)$$
$$+ \tau_{yz}(\cos(x',z)_3\cos(y',y)_3 + \cos(x',y)_3\cos(y',z)_3)$$
$$+ \tau_{zx}(\cos(x',x)_3\cos(y',z)_3 + \cos(x',z)_3\cos(y',x)_3)$$

for a total of nine equations and six unknowns. Two solution methods for this equation set are available. The first is a set of six equations which can be selected and solved simultaneously; the second is a least squares regression. The six equations which provide the best conditioned solution matrix are the σ_x and σ_{xy} relationships derived in each of the three bore holes. This selection is based on the geometric constraint placed on the σ_y relation by setting the cos(y'z) term to zero. It should be noted that the selection of these six equations is based purely on the geometry chosen in this particular development. A least squares evaluation would provide a solution based on all nine equations. The

basis of the technique is the determination of a solution set which produces the minimum residual, or sum of the squares of the differences, between the calculated and measured solutions.

The use of three bore holes provides an accurate means of determining the stress field on the baseline coordinate system. The least squares regression is preferable under field conditions because it reduces the effects of measurement error. Determination of the far-field principal stress magnitude and orientation can be accomplished using Equations 10 through 20.

DEVELOPMENT OF BIAXIAL TESTING TECHNIQUE

A new biaxial testing technique was devised to support the three-dimensional stress transformation theory. The objective was a technique that would operate independently of material properties, and in anisotropic environments, to determine the biaxial stress field magnitude and orientation. Two steps are employed: a radial stress application similar to the initial test performed by Klostermann (1984), and a line load test sequence.

The radial stress device was used to initiate a crack to determine the orientation of the localized principal stress field and the magnitude of the minimum stress concentration. The line load device was used to apply load in the direction of the crack to determine a second stress concentration. This test sequence provides adequate information to determine the orientation and magnitude of the biaxial stress field surrounding the bore hole.

Radial Stress Application

The principle of induced fracturing (Figure 5) is to load the interior of a bore hole with a sufficient radial stress to create a fracture. The creation of a fracture is determined by ultrasonic travel time measurement around the bore hole. Several potential scenarios exist, depending on the condition of the rock after the bore hole is drilled.

If the bore hole is in isotropic, unfractured rock, the application of radial stress will overcome the minimum resistance, defined as the sum

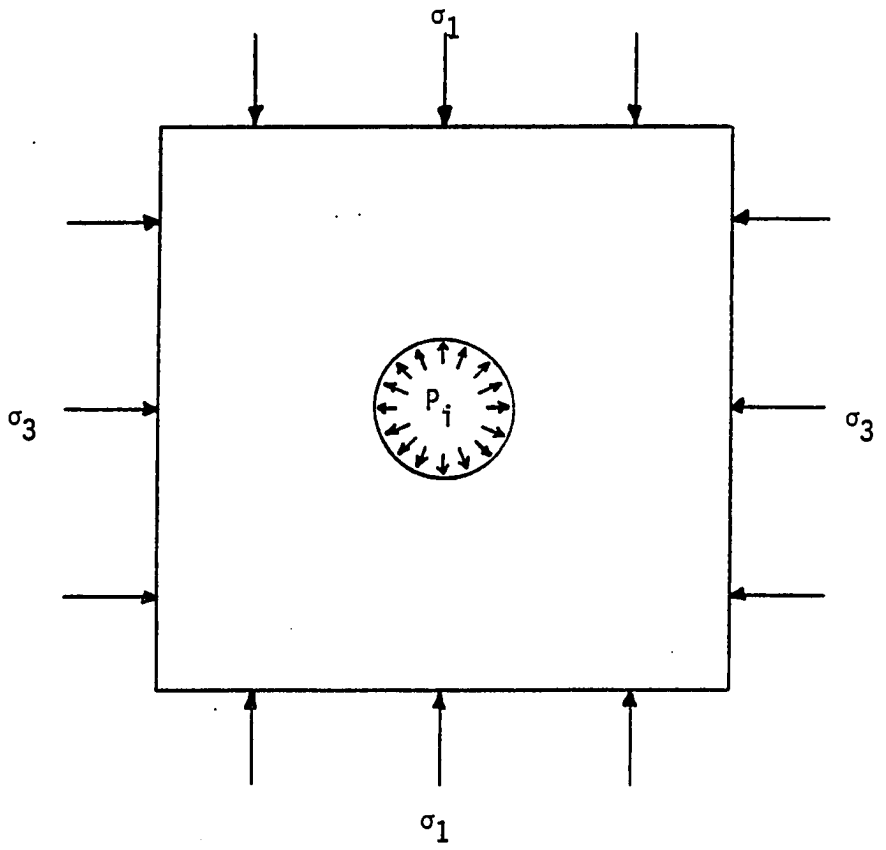

Figure 5: Radial load application

of the minimum radial stress concentration plus the tensile strength of the rock. The resulting radial stress from the first loading is defined by,

$$Pi = T + 3\sigma_2 - \sigma_1 \tag{48}$$

where Pi = internal radial stress,

T = tensile strength of the surrounding rock,

σ_1 = major biaxial principal stress, and

σ_2 = minor biaxial principal stress.

After inducing the initial fracture, the pressure is released and the crack closes. Pressure is then reapplied to reopen the existing crack, yielding the relationship,

$$Pi = 3\sigma_2 - \sigma_1. \tag{49}$$

If the bore hole is situated in anistropic rock, the assumption of the direction of initial fracture in the previous scenario is invalid. In this case, the pressure required to develop a fracture would be the minimum of,

$$Pimin = (f(Ti,\theta) + \sigma_1(1-2\cos 2\theta) + \sigma_2(1+2\cos 2\theta)) \tag{50}$$

where $f(Ti,\theta)$ is the tensile strength of the rock dependent on the position around the bore hole. Thus, the pressure required to reopen the crack would be

$$Pi = \sigma_1(1-2\cos 2\theta) + \sigma_2(1+2\cos 2\theta) \tag{51}$$

where θ corresponds to the position of the crack opened upon initial pressurization.

Another possible scenario is the existence of a crack through the bore hole prior to the initial pressurization. The effect of the preexisting crack is dependent on its orientation. If the preexisting crack is tangential to the axis of the bore hole, the result would be identical to the isotropic case, i.e., the crack would have no effect. If the crack is parallel to or inclined from the bore hole axis, the anisotropic scenario is appropriate because the opening occurs along the path of least resistance. In the case of preexisting cracks, the results from initial and second pressurizations would be similar.

If, after releasing pressure the crack stays open, the relationship between the localized biaxial principal stresses is,

$$\sigma_1 > 3\sigma_2. \tag{52}$$

as indicated by ultrasonic travel time.

In summary, the radial stress portion of the testing technique can yield several possible outcomes, depending on rock conditions. In isotropic homogeneous rocks, where the major biaxial principal stress is less than three times the minor biaxial principal stress, the test determines the tensile strength of the rock as well as the minimum stress concentration. In anisotropic rock, a minimum sum of tensile strength and stress concentration is determined, as well as the value of the stress concentration at the point of fracture. Finally, when the major principal stress is greater than three times the minor principal stress, the test yields a value for the minimum combined value of tensile strength and stress concentration.

Line Load Application

The stress distribution resulting from a directional load (Figure 6) can be described using relationships developed by Jaeger and Cook (1976),

$$\sigma_\theta = p - \left(\frac{4p\alpha}{\pi}\right) \tag{53}$$

where $-\alpha<\theta<\alpha$ or $\pi-\alpha<\theta<\pi+\alpha$

and

$$\sigma_\theta = -\frac{4p\alpha}{\pi} \tag{54}$$

where $\alpha<\theta<\pi-\alpha$ or $\pi+\alpha<\theta<2\pi-\alpha$.

The tangential stress, σ_θ, on the wall of the bore hole in between the loading platens is constant and depends on the magnitude of the applied load, P, as shown in Equation 54.

The state of stress under the loading platens is dependent on the size of the platens themselves, with the resulting tangential stress being compressive, if α is less than 45^o. All work for this project employed loading platens having contact angles (2α) of less than 90^o; therefore, the tangential stress under the loading platen is compressive.

Possible existing conditions, as discussed in the section on radial stress, include isotropic and homogeneous, anisotropic (both due to material and preexisting fractures), and stress conditions that fail to close the fracture upon the release of radial stress. While the effect of line loading is well defined for much of the bore hole surface, it should be noted that stress concentrations at isolated locations may arise due to contact abnormalities. The highest contact stress concentrations will most likely be at the edges of the platen, although some may be encountered anywhere along the contact surface.

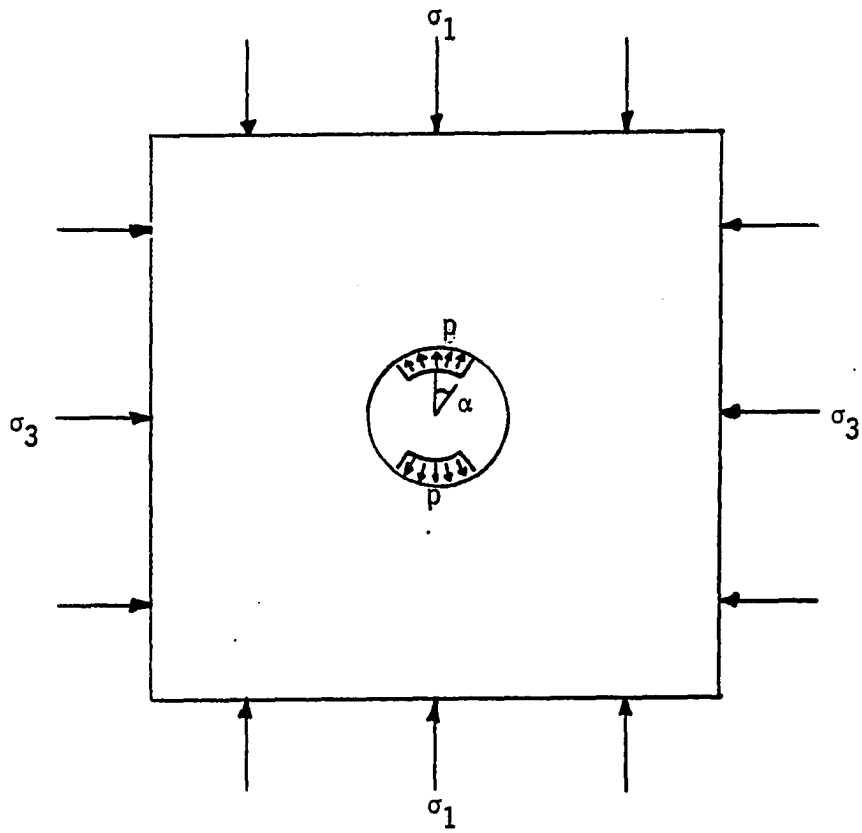

Figure 6: Line load application

In the isotropic homogeneous case, application of a line load perpendicular to the initial fracture will cause cracks to occur at the edges of the platens, because the minimum stress concentration in the portion of the bore hole loaded in tension occurs at these locations. The equation defining this fracture is,

$$\frac{4p\alpha}{\pi} = Ti + \sigma_1(1-2\cos 2\theta) - \sigma_2(1+2\cos 2\theta) \qquad (55)$$

where p = the applied stress and

α = one-half the platen angle, assuming centering over the initial crack.

After load release, the pressure required to reopen the crack is given by

$$\frac{4p\alpha}{\pi} = \sigma_1(1-2\cos 2\theta) + \sigma_2(1+2\cos 2\theta). \qquad (56)$$

To alleviate the effects of contact stress concentrations, the load platens could be rotated slightly after the initial failure to provide a homogeneous stress field in which to reopen the crack; this would provide the same calculated stress level but would remove any effects of contact stress concentrations on the crack opening. With the results of the radial and line load tests, Equations 24 and 31 could then be used to determine the magnitudes of the biaxial principal stresses. The initial fracture direction from the radial test shows the orientation of the principal stress field.

In anistropic rock, the initial crack occurs at the minimum of the function of tensile strength plus tangential stress concentration (Equation 50). A line load test oriented in the direction of this initial fracture could thus produce two results: one possibility is that the sum of tensile strength and stress concentration is a minimum at the platen

edge, causing the test to appear identical to the isotropic case; the other possibility is that the sum of stress concentration and tensile strength has a minimum value somewhere between the load platens, as indicated by the resulting fracture, suggesting that the initial fracture was due to anisotropic conditions surrounding the bore hole. Anisotropic conditions may not be detected with the initial radial and line load tests, so a third test using the line load device should be performed at a different location in the bore hole to ensure detection of anistropy. If isotropic conditions are indicated by the initial tests, the relationship

$$\sigma_\theta = \sigma_1(1-2\cos 2\theta) + \sigma_2(1+2\cos 2\theta) \qquad (57)$$

can be used to predict the stress concentration determined from the third test. When anisotropic conditions are indicated by the initial tests, the results from the third test can be used to solve Equation (57) for σ_1, σ_2, and θ. The use of one radial test and two line-load tests assure the accurate determination of the biaxial stress field surrounding the bore hole, independently of rock strength.

In test cases where a preexisting fracture was encountered in the radial portion of the examination, the line loading test procedure could be modified to provide additional information. As shown in Figure 7, the loading platens could be aligned so one edge of the platen was near the existing crack; the subsequent loading would cause compression of the existing crack and stress the remainder of the bore hole wall. If the minimum stress concentration was anywhere other than at the point of the existing crack, the crack created in the line loading procedure would

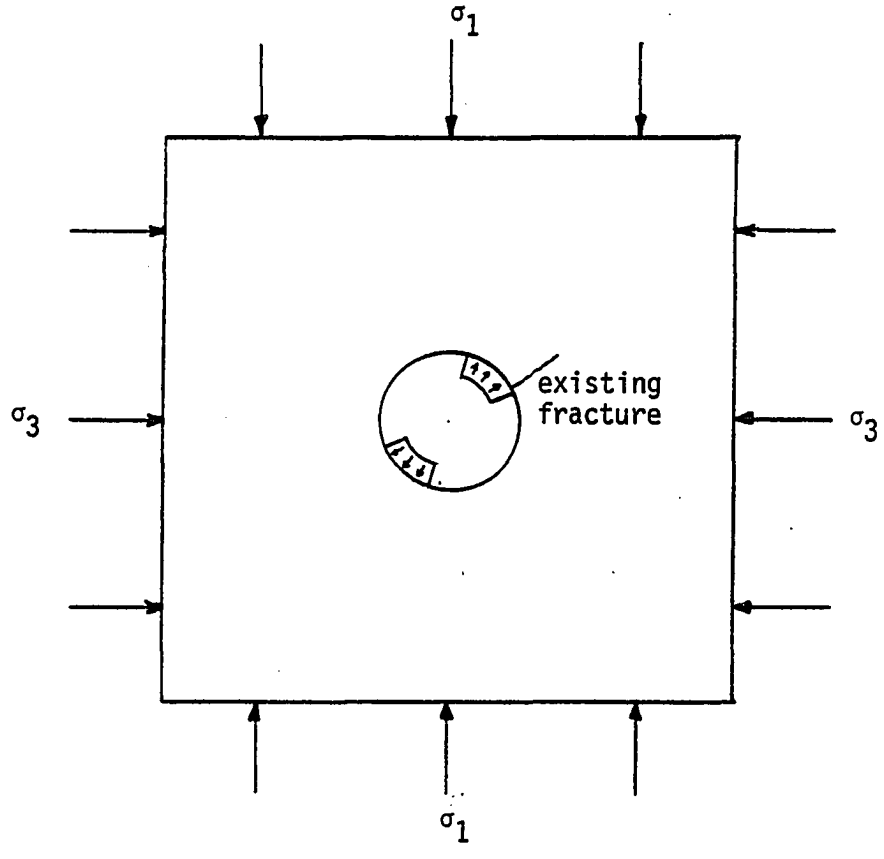

Figure 7: Alignment of line load platens with a preexisting fracture

reflect the location of this minimum stress concentration, due to the symmetrical nature of the stress concentrations around the bore hole. If multiple preexisting fractures are located at various points around the bore hole perimeter, equivalent pressures will be required for both pressurizations of the line load test.

Finally, under the stress conditions that fail to close the crack during the radial stress test, the line load test can be performed in the direction of the initial crack. To assure crack closure under line loading, the required platen angle, α, is

$$\alpha = \tfrac{1}{2}\cos^{-1}\frac{\sigma_1+\sigma_2}{2(\sigma_1-\sigma_2)} \quad . \tag{58}$$

Given a platen of sufficient size, the line load portion of the test would provide a measure of both the tensile strength and a second stress concentration. Therefore, combining the radial and line load tests would allow calculation of the orientation and magnitude of the localized biaxial principal stress field.

EXPERIMENTAL EVALUATION

The purpose of the experimental effort here reported was to determine the performance of the biaxial testing technique under laboratory conditions in a known biaxial stress field.

Experimental Design

Biaxial tests were conducted in 12 x 12 x 6 inch cement mortar blocks, having a one-and-one-half inch bore hole. Biaxial load was applied through platens having independent hydraulic systems to provide a range of stress conditions. Ultrasonic crack detection was accomplished using a set of compression wave transducers mounted on adjacent sides of the bore hole. This testing apparatus is shown in Figure 8. The change in travel time is plotted as a function of load (Figure 9). The initiation of a fracture is defined by a sharp change in the slope.

The radial stress device (Figure 10) is a hollow cylinder cast from Devcon rubber about 1.45 inches in diameter and 6 inches long. Extension of the hydraulic cylinder compresses the rubber and applies radial stress to the bore hole wall. The relationship of radial stress to hydraulic pressure was determined in a pipe section equipped with strain gages (Klostermann, 1984).

The line load device (Figure 11) consists of two steel platens, 1.25 inches wide by 6 inches long, with their outer faces having a radius of 0.75 inches. Load is applied with two opposing wedges mounted on a 0.75 inch threaded rod with a hollow stem hydraulic cylinder. Calibration of

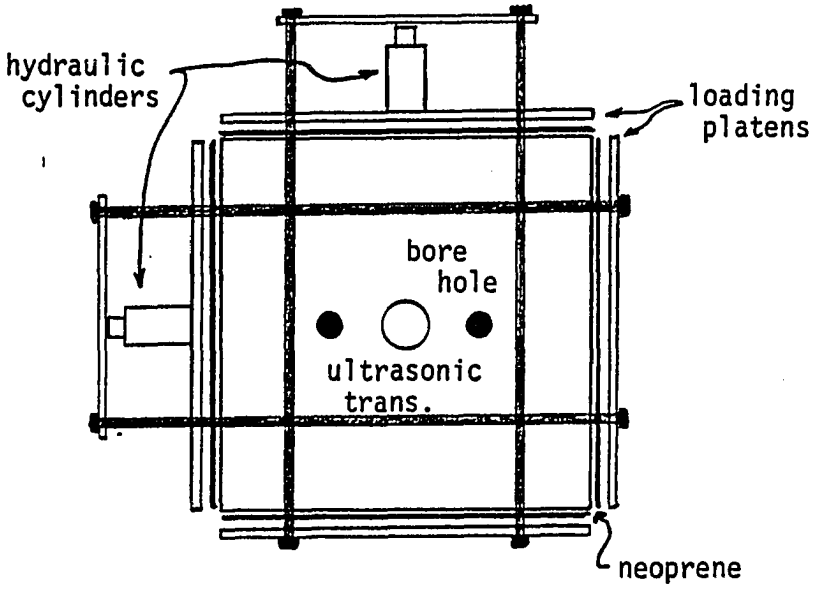

Figure 8: Biaxial test setup

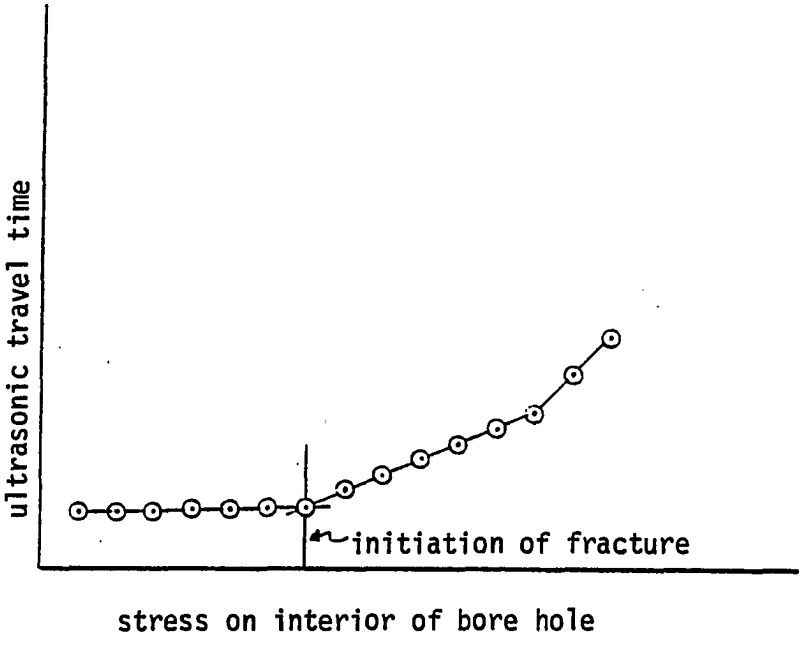

Figure 9: Ultrasonic travel time versus load

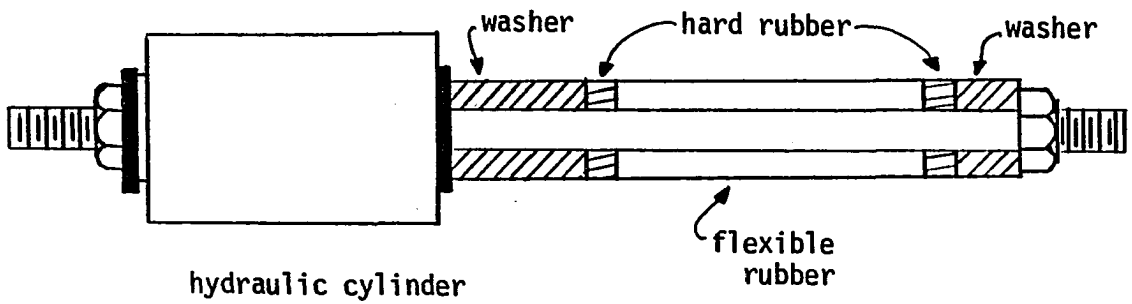

Figure 10: Radial stress device

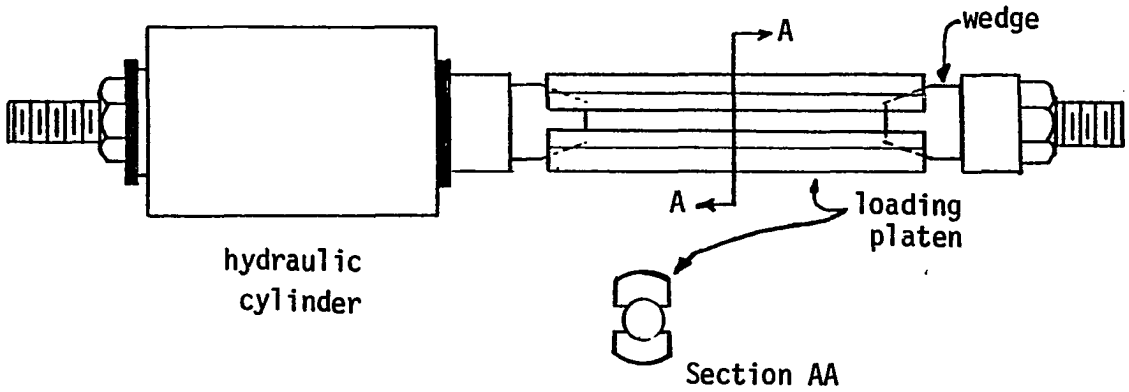

Figure 11: Line load device

the relationship between load and line pressure was achieved against a stiff electronic load cell.

Experimental Results

Line load performance evaluation was the first experimental task. A test specimen was loaded to achieve a 30 psi minimum tangential stress, and the line load device oriented in the minor principal stress direction. Upon loading to failure, the crack direction was parallel to the major principal stress, demonstrating that the stress field created by the line load platens was relatively constant throughout the unloaded portion of the bore hole circumference.

A series of tests were initiated according to the methodology specified in the section on Biaxial Testing Technique. The radial stress device was used both to create the initial fracture and to determine the minor tangential stress concentration upon repressurization; this portion of the test performed adequately. The line load was then inserted parallel to the initial failure and pressurized to create a second fracture. Throughout the first pressurization of the line load device the ultrasonic travel time increased slowly, indicating tensile stress on the existing fracture. After subsequent tests, some of which showed no travel time rise, it was determined that surface roughness of the bore holes caused localized tensile forces on the preexisting crack which overcome the compressive stress field. It should be noted that the ultrasonic probes in these tests were mounted diagonally to the bore

hole, so that any crack opening would affect the travel time. Travel time variation was encountered during line loading; therefore, the ultrasonic probes were moved parallel to the direction of the initial radial stress failure for the line load test. This procedure reduced the influence of the initial crack and improved the failure definition afforded by the test.

Results from biaxial testing are presented in Table 1. The theoretical stress concentrations represent the minimum stress concentration,

$$\sigma_{\theta \min} = 3\sigma_2 - \sigma_1 \tag{59}$$

for the radial stress tests, and the stress concentration at the edge of the line loading platens is defined by

$$\sigma_\theta = 1.778\sigma_1 + 0.2224\sigma_2 \tag{60}$$

unless otherwise noted. All biaxial tests were accomplished prior to visible failure of the block to maintain a homogeneous biaxial field. Visible failure is defined by crack extension to the biaxial loading platens. The test specimens initially used to determine fracture direction are not included in Table 1 because ultrasonic data were not taken.

Blocks 1 and 2 (Table 1) were loaded in the manner initially described in the section on Biaxial Testing Technique. The radial stress was applied until a fracture was detected, then was reapplied to determine the minimum stress concentration. In Block 1, the confining pressure was varied during the radial stress portion of the test to show the performance of the radial stress device. After radial stress testing in Blocks 1 and 2, the line load device was loaded in the postulated direction of the initial fracture until a rise in ultrasonic travel time was

Table 1. Biaxial test results

Block #	Test type	1	2	Theoretical stress conc	Measured stress	Error	Comments
1	Rad	108	81	136 + T	1892.8		
1	Rad	108	81	136	155	+14%	
1	Rad	108	81	136	126	- 7%	
1	Rad	108	75	116	117	+ 1%	
1	Rad	108	75	116	108	- 7%	
1	Rad	165	73	53	46	-13%	
1	Rad	165	73	53	46	-13%	
1	RAD	165	73	53	40	-25%	
1	LL	166	81	313 + T	1999		In dir. of initial failure
1	LL	166	81	313	307	- 2%	
2	RAD	146	91	128 + T	1912		
2	RAD	146	91	128	126	- 2%	
2	LL	146	91	280 + T	1898		In dir. of initial failure
2	LL	146	91	280	272	- 3%	
2	LL	146	91	280	307	+10%	
3	LL	156	83	93 + T	1927		In dir - 2
3	LL	156	83	93	93	0	
3	LL	156	94	128	130	+ 2%	
3	LL	162	86	307 + T			Lost Ultrasonic probe
3	LL	162	86	307	293	- 5%	In dir of initial failure
3	LL	162	80	306	307	0	
3	LL	162	114	314	341	+ 9%	
4	RAD	133	63	56.3 + T	2142		
4	RAD	133	63	56	50	-11%	
4	RAD	133	63	56	88	+57%	
4	RAD	133	63	56	21	-63%	
4	LL	133	63	56	54	- 4%	Tangential to existing crack
4	LL	133	116	215	209	- 3%	

Table 1. continued

Block #	Test type	σ_1	σ_2	Theoretical stress conc	Measured stress	Error	Comments
5	RAD	104	52	52 + T	1950		
5	RAD	104	52	52	42	+19%	
5	RAD	116	33	17			Constant inc. in time
5	LL	116	82	130	174	+34%	
6	LL	133	99	166	155	- 7%	in dir. of σ_2
6	RAD	133	99	166	174	+ 5%	
6	RAD	133	99	166	136	-18%	
6	RAD	133	99	166	130	-22%	

observed. The blocks were then reloaded to determine the stress concentration at the failure point. After testing was completed, both blocks were loaded to visible failure, Block 1 with both the radial and line load devices, and Block 2 with the line load device only. Visible failures occurred at the minimum stress concentration of block 1 and at the edge of the line loading platens in both Blocks 1 and 2.

In Block 3, the line loading device was used exclusively to determine both stress concentrations. The initial load was applied in the σ_2 direction, and the minimum stress concentration determined; the line load platens then were rotated 90^0 and a second test performed. Finally, the line load was applied parallel to the σ_1 direction to visibly fail the specimen, again with the crack occurring at the edge of the line load platen.

Blocks 4, 5, and 6 were tested with a single crack in the direction of σ_1 to evaluate the performance of both devices. In Block 5, a stress field was applied to develop a tensile minimum stress concentration. Testing with the radial stress device showed a constant increase in ultrasonic travel time with load.

Several trends were evident in the deviation of measured stress concentrations from the theoretical values. In Blocks 1, 4, and 5, the radial stress device proved very erratic when used with minimum stress concentrations of less than 100 psi. The radial stress device itself could be the cause of this error; the rubber must undergo axial compression to apply radial stress, so the surface characteristics of the bore hole could have a marked effect on the actual pressure applied. It can

be seen throughout the testing that the radial stress device generally tends to under-predict the minimum stress concentration; possibly this results from stress concentrations near the washers on each end of the rubber cylinder.

The performance of the line loading device in all tests except the test of Block 5 predicts to within 10 percent the theoretical stress level. Direct comparison with the radial stress device in Block 4 demonstrates the superior performance of the line load device.

In summary, the combination of line load and radial tests provides an accurate test method to determine the biaxial stress field around a bore hole. The line load test is capable of functioning with a preexisting fracture and provides a nearly constant tangential stress field in the unloaded section of the bore hole. The variability of the radial stress device is attributed to the rubber loading mechanism, though the device provided consistent performance in fracturing at the minimum tangential stress location.

A NEW CONCEPT FOR UNDERGROUND TESTING

The theoretical and experimental work reported to this point has relied on surface measurements of ultrasonic travel time to determine fracture initiation; visible specimen failure was studied to determine fracture orientation. Radial and line loading devices proved capable of predicting the biaxial stress field; the relationship between the biaxial stress field and the true principal stress field also was developed. Therefore, the applicability of this work to underground testing lies in the ability to perform biaxial tests within the confines of a bore hole.

Biaxial Testing

Ultrasonic determination of crack initiation in a bore hole has recently been made feasible with the development of thin film piezoelectric substrates (Kyner Piezo Film, 1986). The thin film substrates have inadequate thickness to generate a compression wave of sufficient amplitude for use in rock but produce adequate voltage output to be used as a receiver. Thin film piezoelectric substrates are available in thicknesses from nine to 110 microns. In this work, a transducer 28 microns thick, one-sixteenth of an inch wide, and one inch long was chosen to guarantee an electrical output sufficient to be accurately and consistently detected. The transducers respond to both compression and shear waves.

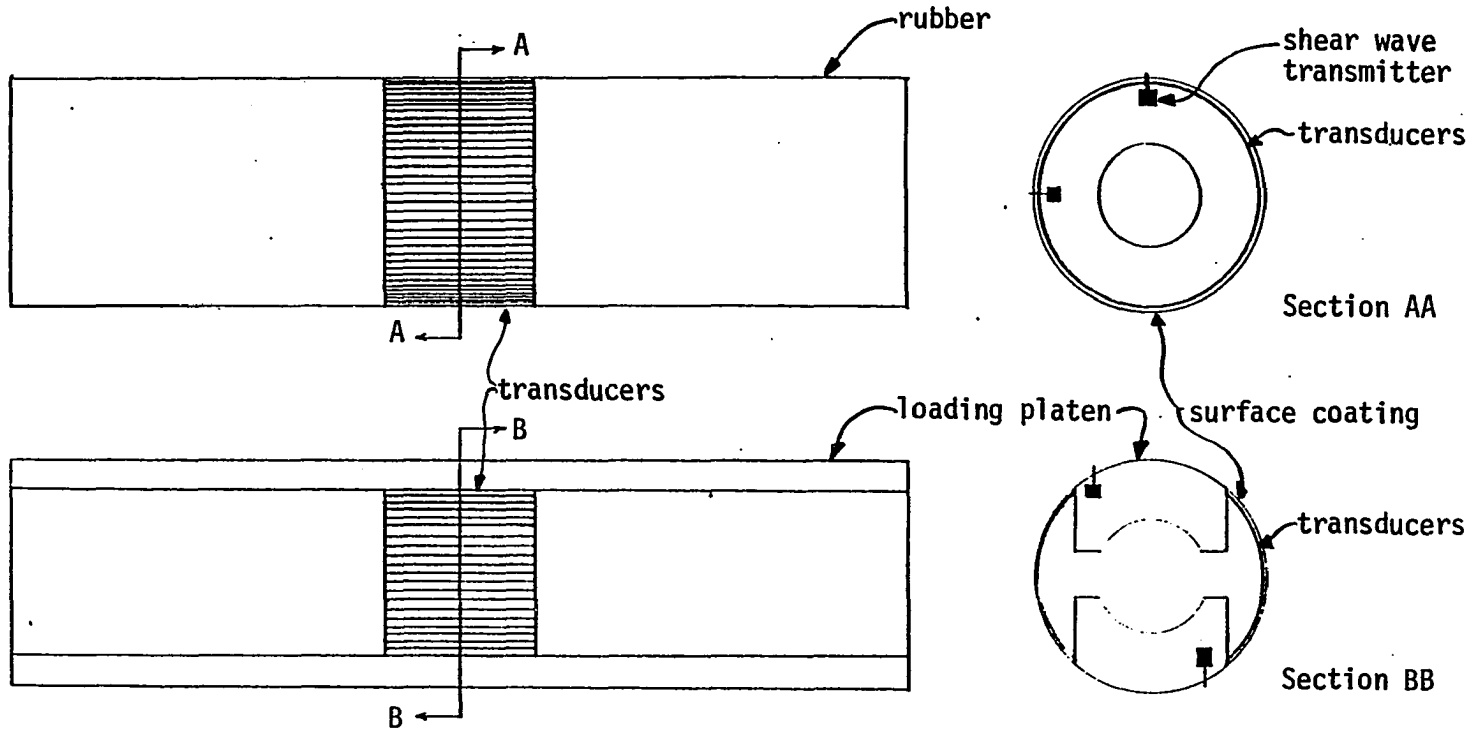

Figure 12: Proposed underground instrumentation

Instrumentation of the biaxial test requires a transmitter and a series of receivers mounted around the circumference of the radial stress device and also in the free space on each side of the line load device (Figure 12). The receivers mounted around the radial device each receive signals until a crack forms. The change in ultrasonic travel time to the receiver immediately adjacent of the crack indicate the location of the fracture. Crack detection for the line load test involves measurement of the portion of bore hole circumference between the loading platens. Again, crack location is determined by the change in ultrasonic travel time to one of the receivers. In both cases, more than one receiver will reflect time changes; the one closest to the transmitters will identify the position of the crack. Given the one-sixteenth of an inch width of the receivers, an angular resolution of five degrees is practical in a one and one-half inch bore hole. Larger diameter bore holes, as are used in deep hole testing, would allow a greater angular resolution. Given the five degree resolution of the transducer system and the reliability of the biaxial stress determination technique, an underground testing scheme as outlined in the Biaxial Testing Technique section would be feasible.

In review, for the isotropic-homogeneous case, the local biaxial stress field's magnitude and orientation is determined from the radial stress application, using Equation 35, and from the subsequent line-load test, whih uses the relationship derived in Equation 41. In cases with preexisting fractures, after determination of the stress concentration at the existing flaw, the line-load device can be employed with the edge of

the platen lying in the direction of the initial flaw. The orientation of the resulting fracture then would indicate the minimum stress concentration. The biaxial principal stress field then could be determined from the results of the two tests.

In cases where a tensile minimum stress concentration is encountered, a series of two line load tests would be required to determine the magnitude of the biaxial stress field. This testing could be accomplished either by using two widths of line load devices or by displacement and subsequent rotation of the line load device in the bore hole to determine a second stress concentration.

In anistropic conditions, a third test with the line load device is required to completely determine the biaxial stress field. With the results of the radial stress and the two line load tests, the three independent relationships developed using Equation 57 can be solved simultaneously to determine the magnitude and orientation of the principal stress field.

The biaxial test method allows the resolution of fracture location to within five degrees and may be used to operate under a variety of conditions which commonly occur underground. It is important to note that while preexisting fractures and tensile minimum stress concentrations are detectable with the test, anistropic conditions are not always discernible. For this reason, it would be a sound practice to perform a third test with the line load device to check the orientation of the minimum stress concentration.

Triaxial Testing

A baseline coordinate system is required to perform an underground test (Figure 3). Three bore holes are then drilled into the undisturbed strata and biaxial tests performed in each bore hole. The biaxial data are then transformed to determine the biaxial stress field $\sigma_{x'}$, $\sigma_{y'}$, and $\sigma_{xy'}$ for each bore hole. To determine the complete stress field for the baseline coordinate system, biaxial data from the three bore holes can be transformed using Equations 39 through 47. Finally, determination of the magnitude and orientation of the principal stress field is accomplished using Equations 10 through 20.

A numerical example illustrating the solution process is outlined in Appendix A. Two methods are available for solving the nine equations generated by the tests in the three bore holes. To aid in this process, a computer program in BASIC is supplied in Appendix B. The program has inputs for biaxial data generated in three bore holes; the orientation, θ, is related to the x' axis.

CONCLUSIONS

1) A method that allows determination of the far field principal stress from biaxial measurements taken in three bore holes at random orientations was developed.
2) The direction cosines can be easily calculated using spherical coordinates which relate bore hole orientation and biaxial fracture angle to the baseline coordinate system, which uses compass and gravitational references.
3) A new biaxial stress measurement technique employing radial and line load devices in connection with ultrasonic crack detection was developed. This measurement technique is capable of stress determination in bore holes with preexisting fractures, anisotropic rock, and tensile minimum stress concentrations.
4) The biaxial test is readily adaptable to underground testing using thin film piezoelectric substrates.
5) In addition, a convenient method to determine the triaxial principal stress field from biaxial data taken from three bore holes is provided in the computer solution, Appendix B.

RECOMMENDATIONS

A biaxial testing technique and a method to determine the triaxial principal stress field from biaxial data have both been developed. Therefore, implementation of the testing scheme requires only the development of instrumentation for underground ultrasonic measurements. It is recommended that:

1) Thin-film piezoelectric receivers be fitted to both radial and line load devices.
2) Ultrasonic shear wave transmitters be developed for both devices; the use of shear waves will allow greater measurement precision in wet holes.
3) An electronic timer be developed to mount on the loading devices, allowing ultrasonic travel time to be measured within the bore hole and transmitted digitally to the surface.

Considering the loading devices used in this work, it is further recommended that:

4) Loading mechanisms be evaluated for underground performance because a hydraulic system using down hole load devices may be more appropriate to underground than the surface loading technique used in this work.

Finally, it is recommended that:

5) Large-scale triaxial testing be undertaken to assay the performance of the entire system in a variety of materials. This large scale testing would allow complete quantification of the accuracy of the testing program.

ACKNOWLEDGMENTS

I would like to extend my heartfelt thanks to Dr. John Pitt for having provided the opportunity and guidance in this and a number of other projects. I would also like to thank Dr. Handy for his patient endurance of half-baked ideas, and for his knowing smile; Dr. Zachary for his enthusiasm, which made this and other projects very enjoyable, and Dr. Lemish and Dr. Nordlie for providing valuable advice on my graduate committee.

I would like to thank Suzanne, who provided not only the support but the inspiration to complete this project and many others. Her steadfast patience has provided the primary impetus for this project.

Finally, I would like to acknowledge the Mining and Mineral Resources Institute and the U.S. Bureau of Mines for partially sponsoring this research.

BIBLIOGRAPHY

Box, G. E. P., W. G. Hunter and J. S. Hunter. Statistics for Experimenters. New York: John Wiley and Sons, Inc., 1978.

Bredehoeft, J. D., R. G. Wolff, W. S. Keys and E. Shuter. "Hydraulic Fracturing to Determine the Regional In Situ Stress Field, Piceance Basin, Colorado." Geological Society of America Bulletin, 87 (1976), 250-258.

Burlington, R. S. Handbook of Mathematical Tables and Formulas. New York: McGraw-Hill, Inc., 1973.

Dally, J. W., and W. F. Riley. Experimental Stress Analysis. New York: McGraw-Hill, Inc., 1978.

Fairhurst, C. "On the Determination of the State of Stress in Rock Masses." Society of Petroleum Engineers of AIME, SPE 1062, 1965.

Ford, H., and J. M. Alexander. Advanced Mechanics of Materials. New York: John Wiley and Sons, Inc., 1977.

Friedman, M. "Residual Elastic Strain in Rock." Tectonophysics, 15, No. 4 (1972), 297-330.

Haimson, Bezalel C. "Deep In Situ Stress Measurements by Hydrofracturing." Tectonophysics, 29, No. 1-4 (1975), 41-47.

Hubbert, M. K., and D. G. Willis. "Mechanics of Hydraulic Fracturing." Transactions, AIME, 210, 1957, 153-165.

Jaeger, J. C., and N. G. W. Cook. Fundamentals of Rock Mechanics. New York: John Wiley and Sons, Inc., 1976.

Klostermann, L. A. "State of Stress in Rock by Induced Fracturing." M.S. thesis, Iowa State University, Ames, Iowa, 1984.

Kyner Piezo Film, Publication TR-5-M-5-85-DF101, Pennwalt Corporation, King of Prussia, Pennsylvania, 1986.

Leeman, E. R. "The Measurement of Stress in Rock." Journal of the South African Institute of Mining and Metallurgy, 65, No. 2 (1964), 45-81.

Miller, A. R. Basic Programs for Scientists and Engineers. Berkeley, CA: SYBEX, Inc., 1981.

Panek, L. (Westwater Professor, Department of Mining Engineering, Michigan Technological University, Houghton, Michigan). Personal communication, August 4, 1984.

Pitt, J. M., and L. Klostermann. "In Situ Stress by Pulse Velocity Monitoring of Induced Fractures." Proc. of the Twenty-Fifth Symposium on Rock Mechanics, Northwestern University, Chicago, IL, June 25-27, 1984.

APPENDIX A:

DETERMINATION OF THE TRIAXIAL PRINCIPAL STRESS FIELD

The procedure used to determine the principal stress field from biaxial data may be illustrated by a random principal stress field with magnitudes of:

σ_1 = 1000 psi,

σ_2 = 500 psi, and

σ_3 = 250 psi,

and an orientation to the baseline axis x (east), y (north), and z (up) such that

cos(x'x) = 0.5

cos(x'y) = 0.5

cos(x'z) = -.7071

cos(y'x) = -.7071

cos(y'y) = .7071

cos(y'z) = 0

cos(z'x) = .5

cos(z'y) = .5

cos(z'z) = .7071.

Three bore holes are then drilled at angles of:

Bore hole #1 θ = 25 λ = 45

Bore hole #2 θ = 20 λ = 135

Bore hole #3 θ = 15 λ = 268

Results of the biaxial testing given in Table A-1 show the biaxial principal stresses determined from Equations 49, 56, and the orientation

to the x' axis. Also included on the table are the transformed biaxial stresses calculated from Equations 28 and 29.

Table A-1. Example calculations

Bore hole	σ_1	σ_2	θ	$\sigma_{x'}$	$\sigma_{y'}$	$\tau_{xy'}$
1	917.8	301.8	- 64.30	417.8	801.8	240.8
2	979.3	429.4	+ 10.64	960.5	448.2	-99.8
3	703.7	446.4	- 30.48	637.5	512.6	112.5

The biaxial information along with the direction cosines calculated using Equations 30 through 38 can be employed using Equations 39 through 47 to build the solution matrix, Equation A1

σ_x	.4107	.4107	.1786	.8214	-.5417	-.5417	417.8
σ_y	-.4532	.4532	0	0	-.2988	.2988	240.8
σ_z	.4415	.4415	.1170	-.8830	-.4545	.4545 =	960.5
τ_{xy}	.5	.5	0	1	0	0	448.2
τ_{yz}	.4698	-.4698	0	0	.2418	.2418	-99.8
τ_{zx}	.00114	.9319	.0670	.0651	.5	.0175	637.5

Solving this matrix with a Gauss-Jordan approximation method yields the complete state of stress on the baseline axis,

σ_x = 500 psi
σ_y = 750 psi
σ_z = 500 psi
τ_{xy} = -176.8 psi
τ_{yz} = -176.8 psi
τ_{zx} = 250 psi

Having defined the baseline stress field, Equations 10 through 20 are then solved to determine the magnitude and orientation of the triaxial principal stress field, which in this case is equal to the one selected for this example.

APPENDIX B: COMPUTER SOLUTION

```
10 REM PRINCIPLE STRESS DETERMINATION FROM 3 BORE HOLES
20 DIM D(3,6),J(6),Q(3,3)
30 DIM Z(9),A(9,9),C1(9),Y(9),U(9,9)
40 DIM W(9,1),B(9,9),I2%(9,3)
50 N2%=6
60 N1%=6
70 PI=3.14159
80 REM
90 REM       ENTER DATA FROM 3 BORE HOLES
100 REM
110 FOR I=1 TO 3
120   CLS
130   PRINT "ANGLE FROM BORE HOLE # ";I;" TO Z AXIS =?":INPUT D(I,1)
140   PRINT "ANGLE FROM BORE HOLE # ";I;" TO X AXIS =?":INPUT D(I,2)
150   PRINT "MAJOR PRINCIPLE STRESS FROM BORE HOLE # ";I;" =?":INPUT D(I,3)
160   PRINT "MINOR PRINCIPLE STRESS FROM BORE HOLE # ";I;" =?":INPUT D(I,4)
170   PRINT "ANGLE BETWEEN MAJOR PRINCIPLE STRESS IN BORE HOLE # ";I;" TO X' AXIS =?":INPUT D(I,5)
180 NEXT I
190 FOR J=1 TO 3
200   TH=D(J,1)*PI/180
210   G=D(J,2)*PI/180
220   ANG=D(J,5)*PI/180
230   A(J,1)=(COS(TH)*COS(G))^2
240   A(J,2)=(COS(TH)*SIN(G))^2
250   A(J,3)=(-SIN(TH))^2
260   A(J,4)=2*COS(TH)*SIN(G)*(-SIN(TH))
270   A(J,5)=2*(-SIN(TH))*COS(TH)*COS(G)
280   A(J,6)=2*COS(TH)*COS(G)*COS(TH)*SIN(G)
290   A(J+3,1)=(SIN(G))^2
300   A(J+3,2)=(COS(G))^2
310   A(J+3,3)=0
320   A(J+3,4)=0
330   A(J+3,5)=0
340   A(J+3,6)=2*((-SIN(G))*COS(G))
350   A(J+6,1)=COS(TH)*COS(G)*(-SIN(G))
360   A(J+6,2)=COS(TH)*SIN(G)*COS(G)
370   A(J+6,3)=0
380   A(J+6,4)=COS(G)*(-SIN(TH))
390   A(J+6,5)=(-SIN(TH))*(-SIN(G))
400   A(J+6,6)=COS(TH)*COS(G)*COS(G)+(-SIN(G))*COS(TH)*SIN(G)
410   Z(J)=D(J,3)*(COS(ANG)^2)+D(J,4)*(SIN(ANG)^2)
420   Z(J+3)=D(J,3)*(SIN(ANG)^2)+D(J,4)*(COS(ANG)^2)
430   Z(J+6)=(D(J,4)-D(J,3))*SIN(2*ANG)/2
440 NEXT J
450 A$=" #####.##"
460 B$=" = #####.##"
470 C$="  ######.##"
```

```
480 M1%=8
490 REM
500 REM     SOLUTION OF MATRIX
510 REM
520 GOSUB 690: REM SQUARE UP THE MATRIX
530 GOSUB 860: REM GET THE SOLUTION
540 REM
550 IF (E1%=1) THEN 680
560 PRINT "         SOLUTION"
570 PRINT
580 REM
590 REM     PRINT STRESSES ON BASE LINE SYSTEM
600 REM
610 LPRINT "    THE STRESSES ON THE BASE LINE SYSTEM ARE"
620 LPRINT "       X          Y          Z         Txy        Tyz        Txy"
630 LPRINT "       -          -          -         ---        ---        ---"
640 FOR I%=1 TO N2%
650   LPRINT USING C$;C1(I%);
660 NEXT I%
670 LPRINT""
680 GOTO 1930
690 FOR K%=1 TO N2%
700   U(4,K%)=U(8,K%)
710 Y(4)=Y(8):NEXT K%
720 RETURN
730 GOTO 860
740     A(K%,L%)=0
750     FOR I%=1 TO N1%
760       A(K%,L%)=A(K%,L%)+U(I%,L%)*U(I%,K%)
770       IF K%<>L% THEN A(L%,K%)=A(K%,L%)
780     NEXT I%
790   NEXT L%
800   Z(K%)=0
810   FOR I%=1 TO N1%
820     Z(K%)=Z(K%)+Y(I%)*U(I%,K%)
830   NEXT I%
840 NEXT K%
850 RETURN
860 REM
870 E1%=0
880 I5%=1
890 N3%=1
900 FOR I%=1 TO N2%
910   FOR J%=1 TO N2%
920     B(I%,J%)=A(I%,J%)
930   NEXT J%
940   W(I%,1)=Z(I%)
```

```
950   I2%(I%,3)=0
960 NEXT I%
970 D3=1
980 FOR I%=1 TO N2%
990   B1=0
1000 FOR J%=1 TO N2%
1010     IF (I2%(J%,3)=1) THEN 1100
1020     FOR K%=1 TO N2%
1030       IF (I2%(K%,3)>1) THEN 1870
1040       IF (I2%(K%,3)=1) THEN 1090
1050       IF (B1>=ABS(B(J%,K%))) THEN 1090
1060       I3%=J%
1070       I4%=K%
1080       B1=ABS(B(J%,K%))
1090     NEXT K%
1100   NEXT J%
1110   I2%(I4%,3)=I2%(I4%,3)+1
1120   I2%(I%,1)=I3%
1130   I2%(I%,2)=I4%
1140   REM
1150   IF (I3%=I4%) THEN 1290
1160   D3=-D3
1170   FOR L%=1 TO N2%
1180     H1=B(I3%,L%)
1190     B(I3%,L%)=B(I4%,L%)
1200     B(I4%,L%)=H1
1210   NEXT L%
1220   IF (N3%<1) THEN 1290
1230   FOR L%=1 TO N3%
1240     H1=W(I3%,L%)
1250     W(I3%,L%)=W(I4%,L%)
1260     W(I4%,L%)=H1
1270   NEXT L%
1280   REM
1290   P1=B(I4%,I4%)
1300   D3=D3*P1
1310   B(I4%,I4%)=1
1320   FOR L%=1 TO N2%
1330     B(I4%,L%)=B(I4%,L%)/P1
1340   NEXT L%
1350   IF (N3%<1) THEN 1410
1360   FOR L%=1 TO N3%
1370     W(I4%,L%)=W(I4%,L%)/P1
1380   NEXT L%
1390   REM
1400   REM
1410   FOR L1%=1 TO N2%
```

```
1420     IF (L1%=I4%) THEN 1520
1430     T=B(L1%,I4%)
1440     B(L1%,I4%)=0
1450     FOR L%=1 TO N2%
1460       B(L1%,L%)=B(L1%,L%)-B(I4%,L%)*T
1470     NEXT L%
1480     IF (N3%<1) THEN 1520
1490     FOR L%=1 TO N3%
1500       W(L1%,L%)=W(L1%,L%)-W(I4%,L%)*T
1510     NEXT L%
1520   NEXT L1%
1530 NEXT I%
1540 REM
1550 REM
1560 REM
1570 FOR I%=1 TO N2%
1580   L%=N2%-I%+1
1590   IF (I2%(L%,1)=I2%(L%,2)) THEN 1670
1600   I3%=I2%(L%,1)
1610   I4%=I2%(L%,2)
1620   FOR K%=1 TO N2%
1630     H1=B(K%,I3%)
1640     B(K%,I3%)=B(K%,I4%)
1650     B(K%,I4%)=H1
1660   NEXT K%
1670 NEXT I%
1680 FOR K%=1 TO N2%
1690   IF (I2%(K%,3)<>1) THEN 1870
1700 NEXT K%
1710 E1%=0
1720 FOR I%=1 TO N2%
1730   C1(I%)=W(I%,1)
1740 NEXT I%
1750 IF (I5%=1) THEN 1890
1760 PRINT
1770 PRINT "   MATRIX INVERSE"
1780 FOR I%=1 TO N2%
1790   FOR J%=1 TO N2%
1800     PRINT USING A$;B(I%,J%);
1810   NEXT J%
1820   PRINT
1830 NEXT I%
1840 PRINT
1850 PRINT "DETERMINANT= ";D3
1860 RETURN: REM IF INVERSE IS PRINTED
1870 E1%=1
1880 PRINT "ERROR, THE MATRIX IS SINGULAR"
```

```
1890 RETURN
1900 REM
1910 REM     DETERMINE PRINCIPAL STRESS MAGNITUDE
1920 REM
1930 P1=C1(1)+C1(2)+C1(3)
1940 P2=-(C1(2)*C1(3)+C1(3)*C1(1)+C1(1)*C1(2))+C1(4)^2+C1(5)^2+C1(6)^2
1950 P3=C1(1)*C1(2)*C1(3)+2*C1(4)*C1(5)*C1(6)-C1(1)*C1(4)^2-C1(2)*C1(5)^2-C1(3)*C1(6)^2
1960 T1=.000001
1970 H2=1E-15
1980 REM
1990 F0%=0
2000 J(2)=3
2010 T0%=NOTF0%
2020 C=2
2030 J(1)=0
2040 X=0
2050 IF(E1%=F0%) THEN J(C)=X ELSE GOTO 2140
2060 FOR Z=1 TO C-1
2070 IF ABS(J(C-Z)-J(C))<1 THEN GOTO 2110
2080 NEXT Z
2090 C=C+1
2100 IF C=5 THEN GOTO 2340
2110 I=I+10
2120 X=I
2130 REM
2140 REM START OF NEWTON'S METHOD
2150 REM
2160 E1%=F0%
2170 REM
2180 X1=X
2190 GOSUB 2310
2200 IF (ABS(F1)>H2) THEN 2240
2210 PRINT "ERROR-SLOPE IS ZERO"
2220 E1%=T0%
2230 GOTO 2300
2240 D6=F/F1
2250 X=X1-D6
2260 IF (ABS(D6)>=ABS(T1*X)) THEN 2180
2270 REM
2280 REM
2290 REM
2300 GOTO 2050
2310 F=(X^3)-(P1*(X^2))-(P2*X)-P3
2320 F1=3*(X^2)-(2*P1*X)-P2
2330 RETURN
2340 LPRINT ""
2350 LPRINT " THE PRINCIPAL STRESSES ARE:"
```

```
2360 LPRINT""
2370 LPRINT USING C$;J(2),J(3),J(4)
2380 LPRINT ""
2390 REM
2400 REM DETERMINE PRINCIPAL STRESS DIRECTIONS
2410 REM
2420 FOR Z=1 TO 3
2430   D=J(Z+1)
2440   B=(C1(2)-D)*(C1(3)-D)-(C1(4)*C1(4))
2450   C=(C1(4)*C1(5)-C1(6)*(C1(3)-D))
2460   A=(C1(6)*C1(4)-C1(5)*(C1(2)-D))
2470   D1=((A^2)+(B^2)+(C^2))^.5
2480   Q(1,Z)=A/D1
2490   Q(2,Z)=B/D1
2500   Q(3,Z)=C/D1
2510 NEXT Z
2520 LPRINT " AND THE RESPECTIVE DIRECTION COSINES ARE:"
2530 FOR I=1 TO 3
2540   FOR J=1 TO 3
2550     LPRINT USING "  ##.####";Q(I,J);
2560   NEXT J
2570   LPRINT ""
2580 NEXT I
2590 END
```